Graphical Abstract

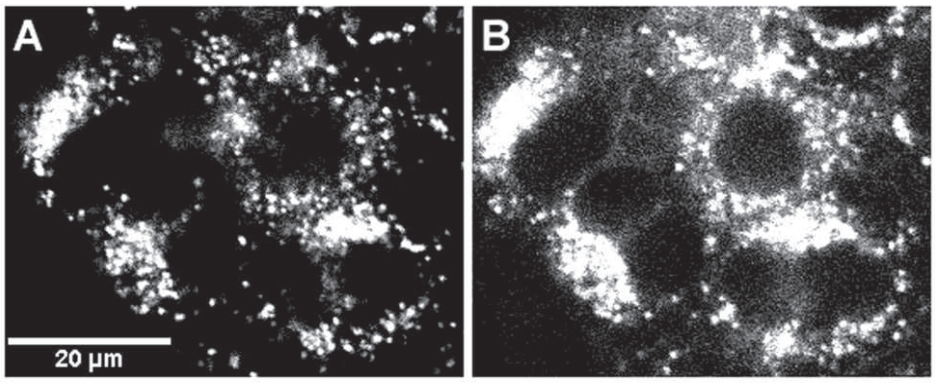

Cellular confocal fluorescence distribution of the Tat peptide-tetraphenyl porphyrin conjugate and its photo-induced redistribution in HN5 carcinoma cells

Manuscript for ELSEVIER journals: Journal of Controlled Release *(Article type: Research Paper)*

Title: Photochemical internalisation of a macromolecular protein toxin using a cell penetrating peptide-photosensitiser conjugate

Authors: Julie, T-W Wang[a] , Francesca Giuntini[b], Ian M. Eggleston[b], Stephen G. Bown[a], Alexander J. MacRobert[a,*]

Institutional affiliations:

[a]: National Medical Laser Centre, Division of Surgery & Interventional Science, University College Medical School, University College London, London, UK

[b]: Wolfson Laboratory of Medicinal Chemistry, Department of Pharmacy and Pharmacology, University of Bath, Bath, UK

*Corresponding author. National Medical Laser Centre, Charles Bell House, 67-73 Riding House Street, London, W1W 7EJ, UK. Tel: +44 (0)2076799019, Fax: +44(0)2078132828

E-mail address: a.macrobert@ucl.ac.uk

Abbreviations: CPP, cell penetrating peptide; DMF, dimethylformamide; DMPC, dimyristoyl phosphatidylcholine; PCI, photochemical internalisation; PDT, Photodynamic therapy; SPPS, solid phase peptide synthesis; Tat, trans-activating transcriptional activator; TFA, trifluoroacetic acid; TPP, TP-porphine.

Abstract

Photochemical internalisation (PCI) is a site-specific technique for improving cellular delivery of macromolecular drugs. In this study, a cell penetrating peptide, containing the core HIV-1 Tat 48-57 sequence, conjugated with a porphyrin photosensitiser has been shown to be effective for PCI. Herein we report an investigation of the photophysical and photobiological properties of a water soluble bioconjugate of the cationic Tat peptide with a hydrophobic tetraphenylporphyrin derivative. The cellular uptake and localisation of the amphiphilic bioconjugate was examined in the HN5 human head and neck squamous cell carcinoma cell line. Efficient cellular uptake and localisation in endo/lysosomal vesicles was found using fluorescence detection, and light-induced,rupture of the vesicles resulting in a more diffuse intracellular fluorescence distribution was observed. Conjugation of the Tat sequence with a hydrophobic porphyrin thus enables cellular delivery of an amphiphilic photosensitiser which can then localise in endo/lysosomal membranes, as required for effective PCI treatment. PCI efficacy was tested in combination with a protein toxin, saporin, and a significant reduction in cell viability was measured versus saporin or photosensitiser treatment alone. This study demonstrates that the cell penetrating peptide-photosensitiser bioconjugation strategy is a promising and versatile approach for enhancing the therapeutic potential of bioactive agents through photochemical internalisation.

Key words: Cell penetrating peptide, Tat peptide, Photodynamic Therapy, PDT, Photochemical Internalisation, PCI

1. Introduction

Photochemical Internalisation (PCI) is a technology developed by Berg and co-workers [1-3], which can enhance drug delivery using light in combination with photosensitisers localised in endo/lysosomal membranes. The technique is aimed at improving the delivery of bioactive agents which become sequestered within endo/lysosomal vesicles and are therefore unable to exert their action upon the target site. With PCI, the light-induced rupture of the photosensitised vesicle membranes enables the agents to reach their intracellular target. The aim of this study was to investigate whether a cell penetrating peptide bioconjugate can be used to enhance drug delivery.

Pharmaceutical agents can suffer from low bioavailability due either to poor cell membrane penetration and/or the lack of water solubility. In tackling this key problem in drug delivery, an active area of research to improving bioavailability is the conjugation of drugs with cell penetrating peptides (CPP), which can enhance the water solubility and cellular uptake of drugs [4]. Two studies independently reported the cell membrane translocation ability of the trans-activating transcriptional activator (Tat), a protein from human immunodeficiency virus type I (HIV-1) [5,6] using the 86-mer Tat or the purified Tat protein. Both Tat proteins were able to enter cultured cells and induce the trans-activation of the viral promoter. The full-length protein was soon characterized as a protein with multiple functional domains [7,8] and the highly basic region which contains six arginine and two lysine in nine residues is assigned to the protein translocation activity [9]. Since then, other natural or designed proteins or peptides have also demonstrated the property of translocation [10]. These proteins and peptides all contain the highly positive charged protein transduction domains (PTDs) or cell penetrating peptides (CPPs) that are responsible for protein transduction, i.e. the translocation process across the cell membrane.

Several approaches to linking pharmaceutical cargos to Tat peptides or other CPPs to overcome the cell membrane barrier have been carried out. To date, Tat peptides have been proven to facilitate the cell entry of various molecules ranging from peptides [11] with molecular weights of hundreds of Dalton to larger structures such as liposomes [12]. The remarkable success of Tat peptides in drug delivery has drawn considerable attention to the mechanisms involved in the internalisation and intracellular delivery. A reduction of cellular uptake was found when Tat

peptides were modified with single deletion or substitution of the core sequence 'GRKKRRQRRR' in the basic domain resulted in the change of charges [13,14]. Diminished cellular uptake indicated the unique highly cationic nature of Tat peptides certainly plays a key role in the cell uptake process, and the direct electrostatic interaction between the positively charged Tat peptides and the negatively charged proteoglycans or glycosaminoglycans on the cell surface is believed to be required in the internalisation mechanism[15,16].

Despite earlier misinterpretations of the uptake mechanism resulting from artefacts caused during the cell fixation procedures, endocytic uptake is the generally recognised mechanism for Tat peptide and most other CPP mediated drug delivery [17,18]. Both lipid raft-mediated caveolar endocytosis and the clathrin-mediated endocytosis have been identified as endocytic routes of Tat-fusion proteins [19,20], in addition to macropinocytosis, a rapid non-specific lipid raft cell uptake pathway [21]. To date, more than 20 Tat-derived short peptides with various modifications at either the N-terminal or the C-terminal ends have been used for delivering drugs into cells [22]. The advantages and versatility of the Tat peptide-mediated drug delivery have also been applied *in vivo*. For example, in a study conducted by Schwarze et al used a Tat fusion protein (120kD) in which β-galactosidase (116 kD) was ligated to the protein transduction domain [23]. After intraperitoneal injection in mice, the conjugate was found to distribute into virtually every organ and even cross the blood brain barrier after 4 hr. These promising results have led to the possibility of Tat peptides being used for *in vivo* drug delivery.

Porphyrins and their analogues constitute the major class of photosensitising agents in photodynamic therapy (PDT), which is a local treatment for both malignant and no-malignant pathologies. Its therapeutic effects arise from the photo-oxidative damage initiated by the photosensitised generation of reactive oxygen species. [24]. As with other pharmaceutical agents, many photosensitising agents exhibit poor bioavailability being either too hydrophilic or conversely too hydrophobic and limited water solubility. Conjugation strategies that modify photosensitisers by linking to certain peptides or proteins with targeting function have been used to improve the selectivity of photosensitiser delivery [25,26]. For example, penetratin coupled to 5-aminolevulinic acid was shown to be taken up by cells and could be successfully converted to photoporphyrin IX via the haem biosynthetic pathway [27]. CPP-porphyrin conjugates have been recently synthesized as photoactive compounds. Sibrian-Vazquenz et al synthesized different porphyrin-peptide conjugates bearing PEG linkers to several targeting sequences including the Tat peptide (48-60) to compare their cellular uptake, subcellular localisation and the phototoxicity *in vitro* [28]. Sehgal et al, from the same group, examined the cellular uptake and phototoxicity of five porphyrin-peptide conjugates using a prostate cancer cell line [29]. Recently we have also shown that a Tat-porphyrin conjugate is effective for antimicrobial PDT [30].

In photochemical internalisation (PCI), the light-induced rupture of the endo/lysosomal membranes enables therapeutic agents sequestered within endo/lysosomes to reach their intracellular target. In contrast to photodynamic therapy, PCI is a site-specific drug delivery technique where the therapeutic action is exerted by the drug itself but not the by photosensitiser or the reactive oxygen species. For example, previous studies in our laboratory have demonstrated successful reversal of doxorubicin drug resistance *in vitro* by PCI [31,32]. Other agents successfully delivered using PCI include siRNA [2] and a peptide nucleic acid (PNA), where the PNA was conjugated to a cell penetrating peptide but not the photosensitiser [33].

Using an *in vivo* rat liver model, we have also demonstrated that PCI-mediated release of low doses of a protein toxin can give enhanced tissue damage [1]. Type I ribosome inactivating proteins (RIPs) such as gelonin and saporin exert a lethal effect on protein synthesis only if delivered into the cytosol, however due to their size they can become sequestered within endo/lysosomes [34]. Enhanced drug delivery of saporin and other RIPs (gelonin) to the cytosol has previously been demonstrated using PCI technology and amphiphilic disulfonated photosensitisers *in vitro* [35-37]. These amphiphilic disulfonated photosensitisers were selected since they exhibit preferential localisation in endo/lysosomal membranes in order to promote the PCI effect. It is important to note that the criteria for selection of a photosensitiser for PCI are

distinct from PDT where localisation in several subcellular compartments may confer an advantage (e.g. in mitochondria) rather than the specific endo/lysosomal localisation required for PCI. Identification and optimisation of new photosensitising compounds for PCI therefore presents a different experimental challenge.

In the present study, we investigated the hypothesis that a Tat-TPP conjugate could be particularly suitable for PCI because of the resulting amphiphilicity conferred by cationic Tat peptide sequence and the hydrophobic porphyrin. Such an amphiphilic structure should favour membrane binding essential for PCI, but retain good water solubility. Photophysical and biological studies of a peptide-porphyrin conjugate were carried out to assess its efficacy for PCI in enhancing intracellular delivery and cytotoxicity of the macromolecular toxin, saporin.

2. Materials and Methods

2.1. Chemicals

Chemical reagents were purchased from Sigma-Aldrich (Gillingham, UK), Fluka (Gillingham, UK), Acros (Loughborough, UK), Lancaster (Lancashire, UK) and Novabiochem (Nottingham, UK). All other solvents were purchased from Fisher Scientific (Loughborough, UK) and used as received. Peptide grade dimethylformamide was purchased from Rathburn Chemicals Ltd. (Walkerburn, UK). Preparative RP-HPLC was performed on a Dionex HPLC system (Leeds, UK) consisting of an Ultimate 3000 WPS autosampler, a P680 preparative pump (HPG), a UVD 170U multiwavelength detector, and a Foxy Jr fraction collector. The purifications were performed on a Phenomenex Gemini 5 µm C-18 (250 x 30 mm) column with a flow rate of 22.5 mL/min. Mobile phase A was 0.1% TFA in water, mobile phase B was 0.1% TFA in acetonitrile. High resolution mass spectrometry was performed using a Bruker MicroTOF autospec ESI mass spectrometer (Coventry, UK). $TPPS_4$ (tetrasulfonated tetraphenylporphine) was supplied by Frontier Scientific (Frontier Scientific Europe, Lancashire, UK). $TPPS_{2a}$ (disulfonated tetraphenylporphine) was a gift from PCI Biotech (Oslo, Norway).

2.2. Synthesis of Tat-TPP conjugate

The Tat-TPP conjugate **2** was prepared by the ligation of the maleoylporphyrin derivative **1** (5 eq) to a HIV-1 Tat 48-57 analogue (1 eq), wherein the peptide was extended at the C-terminus by the tetrapeptide amide GYKC-NH_2 (Fig.1), as used elsewhere [38]. The peptide was synthesised by 9-fluorenylmethoxycarbonyl (Fmoc)-SPPS, and the ligation reaction was performed in solution in DMSO containing pyridine, shielded from light, as recently described by us [30]. The crude product was isolated on a Discovery DSC-18 solid phase extraction cartridge (Supelco, Gillingham, UK). The desired compound was eluted with (5% MeCN-0.1% aq TFA) mobile phase: and lyophilised. **2** was subsequently characterised by high resolution mass spectrometry, and its purity confirmed as > 95% by analytical RP-HPLC. The Molecular Weight of the conjugate is 3869 Da.

2.3. Cell line and cultivation

The experiments in this study were carried out using HN5 human squamous cell carcinoma cells. HN5 cells were obtained from Prof. Michael O'Hare (UCL Dept. of Surgery and Ludwig Institute for Cancer Research, London, UK). Cells were cultured in Dulbecco's Modified Eagle's medium containing 10% FBS (Sigma-Aldrich, Gillingham, UK), 100µM nonessential amino acid, 2mM glutamine (Gibco BRL, Life Technologies Ltd, Paisley, UK) and 500µg/ml Gentamicin (Gibco BRL, Life Technologies Ltd, Paisley, UK). Cells were incubated at 37 °C in a humidified atmosphere containing 5% CO_2.

2.4. Preparation of Tat-TPP conjugate solutions in liposomes

In order to demonstrate that the Tat-TPP conjugate is capable of portioning to lipid membranes, spectroscopic studies were carried out by mixing an aqueous solution of the conjugate with an aqueous dispersion of liposomes. Stock solutions of the Tat-TPP conjugate were prepared by

dissolving the powder in water at a concentration of 100 μM. The aqueous dispersions of DMPC (dimyristoyl phosphatidylcholine, Sigma-Aldrich, Gillingham, UK) liposomes were prepared according to the procedure described by Hope et al. [39]. A film of lipid (total 20 μ moles) was prepared on the inside wall of a round bottom flask by evaporation of $CHCl_3$ solutions containing the required amount of DMPC to obtain the molar percentage mixture. The obtained films were stored in a dessicator overnight under partial evacuation and were then admixed with 1 ml of PBS buffer solution in order to obtain lipid dispersions (12.5 mM). The solutions were vortex-mixed and then freeze-thawed six times from liquid nitrogen to 313 K (40 ºC). Dispersions were then extruded (10 times) through a 100 nm polycarbonate membrane (Whatman Nuclepore, Maidstone, UK). The extrusions were carried out at 307 K (34 ºC), well above the transition temperature of DMPC (297.2 K), using a 2.5 ml extruder (Lipex Biomembranes Inc., Vancouver, Canada).

2.4.1. Photophysical Characterisation

Absorption spectra were measured using a Perkin-Elmer Lambda 25 UV/Vis spectrometer (Perkin-Elmer, Beaconsfield, UK) with quartz cuvettes. Spectra were measured with samples prepared from the stock solution using different solvents, e.g. water, methanol, or deuterated methanol (CH_3OD) (Sigma-Aldrich, Gillingham, UK). The fluorescence emission and excitation spectra of the conjugate in aqueous and liposomal solutions were measured using a LS50B Perkin-Elmer spectrofluorimeter (Perkin-Elmer, Beaconsfield, UK). A front surface excitation/detection geometric configuration was used to minimise self-absorption artefacts.

2.4.2. Fluorescence lifetime measurements

Fluorescence lifetimes were measured using the time-correlated single photon counting method (TCSPC). Dilute solutions in methanol at a concentration of 0.5 μM were employed. The light source was a 405 nm pulsed laser diode (EPL-405, Edinburgh Instruments Ltd., Livingston, UK) with a pulse duration of 90 picoseconds, and 5MHz repetition rate. The fluorescence was detected using a fast multialkali photomultiplier module (model H5773-04, Hamamatsu Photonics UK Ltd, Hertfordshire, UK) via a longpass filter (OG510, Schott, Stafford, UK) and a monochromator (model M300, Bentham Instrument Ltd, Berkshire, UK)**.** TCSPC was carried out using a PC-mounted board (TimeHarp100, PicoQuant GmbH, Berlin, Germany) and lifetimes were derived using FluoFit software (PicoQuant GmbH, Berlin, Germany). The Instrument Response Function (IRF) was obtained from a non-fluorescent scattering Ludox® solution (Sigmal-Aldrich, Gillingham, UK). Optimum fitting with minimisation of the residuals was confirmed using a Chi-squared value $\chi^2 < 1.4$.

2.4.2. Singlet oxygen yield measurements

The singlet oxygen phosphorescence at 1270 nm was detected using time-resolved photon counting from aerated solutions in deuterated methanol (CH_3OD) in quartz cuvettes. For detection in the near-IR, a thermoelectrically cooled photomultiplier (model H10330-45, Hamamatsu Photonics Ltd, Hertfordshire, UK) was used, and emission was collected via a series of lenses from the cuvette in combination with a long-pass and a band-pass filter centred at 1270 nm (Infrared Engineering Ltd, Essex, UK). The solutions were excited using a 532 Nd:YAG laser (Lumanova GmbH, Hannover, Germany) with the beam axis aligned orthogonally to the collection optics. The laser was pulsed at a repetition rate of 3 kHz and a pulse length of 3 ns, giving a mean power of 8mW, and a fast photodiode (1 ns rise time, Becker-Hickl, Berlin, Germany) was used to synchronize the laser pulse with the photon counting detection system. A series of neutral density filters was used to attenuate the laser power. The photon counting equipment consisted of a PC-mounted multiscaler board (model MSA-300, Becker-Hickl, Berlin, Germany) and a pre-amplifier (Becker-Hickl, Berlin, Germany) which gave a resolution of 5 ns per channel. Time-resolved phosphorescence measurements were accumulated by the multiscaler board. The traces were analysed using FluoFit software (PicoQuant GmbH, Berlin, Germany) to extract the singlet oxygen decay lifetime. To calculate the quantum yield the standard zero-time

intercept analysis was used. $TPPS_4$ (tetrasulfonated tetraphenylporphine) was chosen as the reference compound [40,41].

2.5. Cellular uptake of Tat-TPP

HN5 cells were seeded in 96-well plates at $2.5x10^4$ cells/well one day before drug application. For the time-dependent cell uptake experiment, cells were treated with 1μM Tat-TPP added from an aqueous stock solution for various time periods up to 8 hr. For temperature-dependent experiments, all protocols were the same except that the incubations of photosensitisers were performed at 4 ºC or 37 ºC for 1 hr. For the dose-dependent uptake measurement, cells were incubated with Tat-TPP with different concentrations from 0.1 μM to 5 μM for 18 hr. Comparative studies were carried out following the same protocols with 1 μg/ml (1.3 μM) $TPPS_{2a}$ instead. At the selected uptake measurement time points, cells were washed with PBS and incubated in clear DMEM medium (no phenol red; no serum) for fluorescence measurement using a spectrofluorimeter with a fibre-optic attachment designed to record fluorescence from 96 well plates (LS50B spectrofluorimeter, Perkin-Elmer, Beaconsfield, UK).

2.6. Subcellular distribution, post-light redistribution and co-localisation studies using confocal microscopy

HN5 cells were seeded overnight in Petri dishes incorporating a coverslip window on the underside designed for microscopy (FluoroDish™ , World Precision Instruments, Stevenage, UK) and were then incubated with 2.5 μM Tat-TPP for 18 hr. After being thoroughly washed and incubated with fresh full medium for further 4 hr, cells were incubated with clear phenol red-free DMEM for fluorescence microscopy. The cellular distribution and redistribution after 10min light irradiation were observed by confocal microscopy (FluoView FV1000, 60x magnification, NA 1.20, Olympus UK Ltd, Essex, UK). The light treatment was carried out on stage by using the 543 nm laser of the microscope. Fluorescence images were taken during the irradiation process at several time points. For co-localisation studies, after the 18 hr incubation with the Tat-TPP conjugate (2.5 μM), and thrice washing and a further 4 hr incubation with fresh medium, cells were incubated for 30 min with 50 nM LysoTracker Green for lysosomal labelling or MitoTracker Green (Molecular Probes, Paisley, UK) for mitochondrial labelling. Clear medium was again used for live cell imaging using confocal microscopy.

2.7. Phototoxicity of Tat-TPP and its PCI effect in combination with saporin

HN5 cells were seeded at 5000 cells/well in 96-well plates overnight. Cells were treated with the Tat-TPP conjugate (0.05, 0.1 and 0.2 μM) or saporin (Sigma-Aldrich Gillingham, UK) (10, 25 nM) for 18 hr separately. Another three groups of cells were co-incubated with saporin (10, 25 or 50nM) and 0.1μM Tat-TPP. Cells were then washed thrice with PBS and incubated a further 4 hr with fresh full medium. Irradiation was carried out for up to 5 min using a blue LumiSource® flatbed lamp with peak emission c. 420 nm and 7 mW cm^{-2} output (PCI Biotech, Oslo, Norway). Cell viability was determined by means of the standard MTT (3-(4,5-dimethylthiazol-2-yl)-2,5-diphenyltetrazolium bromide) (Sigma-Aldrich, Gillingham, UK) assay 2 days after the light exposure.

2.8. Statistical analysis

Results are presented as mean ± standard deviation (SD). Significant differences were assessed by two-tailed Student's t-test analysis. $p \leq 0.05$ was considered statistically significant.

3. Results

3.1. Spectroscopic studies

The structure of the peptide-porphyrin conjugate is shown in Fig. 1. The lipophilic tetraphenyl porphyrin is coupled via a linker to the Tat peptide, which is cationically charged since the peptide contains several amino groups which will be protonated at physiological pH. The peptide

comprises the core HIV-1 Tat 48-57 sequence, with a C-terminal tetrapeptide extension containing cysteine, as described by Santra et al [38], to allow attachment of a functionalised porphyrin by bioorthogonal thiol-maleimide ligation (see Section 2.2).

With this amphiphilic structure, the bioconjugate should in principle localise well in membranes with the hydrophobic porphyrin localised within the lipid membrane and the cationic Tat sequence residing at the anionic membrane surface. Based on this reasoning it was hypothesized that this bioconjugate would be effective for PCI.

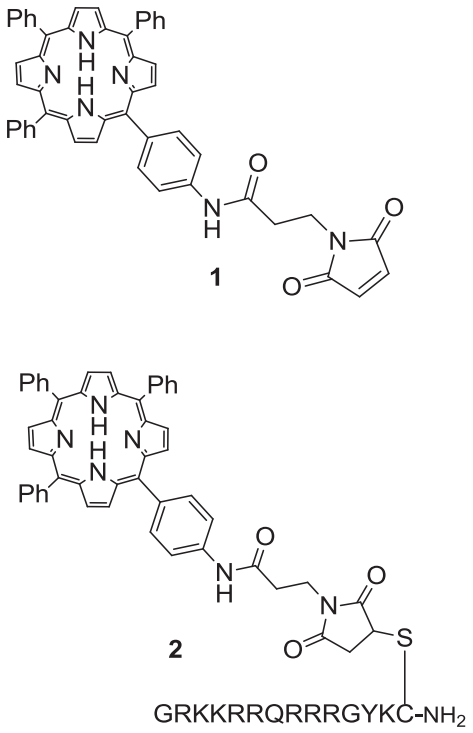

Fig. 1. Structures of modified tetraphenylporphyrin **1** and Tat-tetraphenylporphyrin (Tat-TPP) bioconjugate **2**.

3.2. Spectroscopic analysis of Tat-TPP

Fig. 2 shows the absorbance spectrum of 5 μM Tat-TPP conjugate in aqueous solution (distilled water). The peak absorption of the Soret band was observed at 418 nm. The weaker series of Q band absorption peaks are shown in the inset with the longest wavelength peak in the red at 642 nm (Fig. 2, inset). In methanol, the peak absorption was observed at 414 nm. At this wavelength, the molar extinction coefficient was measured as 2.9 x 10^5 $M^{-1}cm^{-1}$ in methanol.

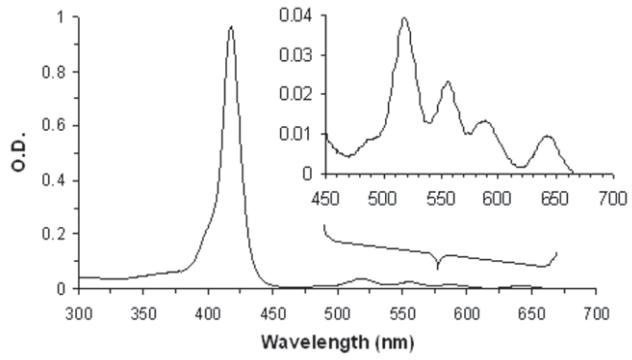

Fig. 2. Absorption spectrum of 5 μM Tat-TPP conjugate in aqueous solution. Inset: the Q band region from 450 nm to 700 nm.

The fluorescence emission and excitation spectra of the Tat-TPP conjugate in aqueous and DMPC liposomal solutions are shown in Fig. 3. Peak fluorescence emission in aqueous solution was detected at 652 nm and 714 nm, and the maximum excitation intensity was at 417 nm ($\lambda_{emission}$ 651 nm). Red-shifted fluorescence spectra were observed in the liposomal solution with peak fluorescence emission detected at 655 nm and 721 nm while the maximum excitation intensity was recorded at 420 nm.

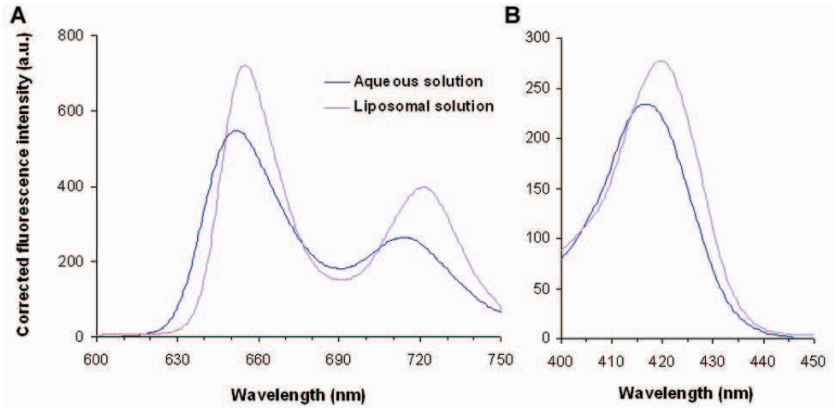

Fig. 3. Fluorescence spectrum of 2.5 μM Tat-TPP in aqueous and DMPC liposomal solutions. A: Emission spectra ($\lambda_{excitation}$ 420 nm); B: Excitation spectra ($\lambda_{emission}$ 651 nm). The emission spectra were corrected for the variation of detector sensitivity with wavelength. Front surface excitation/detection geometry was employed to minimise self-absorption.

3.3 Photophysical studies

In order to minimise dimerisation due to the hydrophobic TPP moiety in the conjugate, methanol was chosen as the solvent for the fluorescence lifetime measurement. For the determination of the singlet oxygen quantum yield, deuterated methanol (CH_3OD) was used. To confirm that the methanolic solutions at the concentrations studied were monomeric, absorption spectra were recorded as a function of concentration. It was necessary to check for the presence of any aggregation because aggregated porphyrins exhibit shorter fluorescence lifetimes and lower singlet oxygen quantum yields. The absorption spectra of the Tat-TPP conjugate were measured in methanol and deuterated methanol and the peak absorbance of the Soret Band (at 414 nm) was found to be linear versus concentration up to 2 μM confirming that Tat-TPP conjugate was present in monomeric form.

3.3.1. Fluorescence lifetime measurements

The measurement of the fluorescence lifetime of Tat-TPP in methanol (0.5 μM) exhibited a good mono-exponential decay fitting with the value of 8.7 ns (Table 1). A slightly longer value was observed in deuterated methanol (10.7 ns) as expected due to the isotope effect. For comparison, the lifetime of $TPPS_4$ was measured as 9.7 ns in methanol.

3.3.2. Singlet oxygen quantum yield

The quantum yield of the Tat-TPP conjugate was measured in comparison with that of a known reference compound, $TPPS_4$ (Φ_Δ = 0.7 in CH_3OD) [40,41]. Using standard zero-point intercept analysis with optically matched solutions [42], the singlet oxygen quantum yield of Tat-TPP was calculated as 0.54.

Table 1 summarizes the photophysical properties of the Tat-TPP conjugate.

	dH_2O[a]	MeOH[b]	DMPC[c]	MeOD[d]
$\lambda_{abs\ Soret}$ (nm)	418	414	-	-
$\lambda_{abs\ Q}$ (nm)	642	645	-	-
λ_{ex} (nm)	417	-	420	-
λ_{em} (nm)	652, 714	-	655, 721	-
τ_F (ns)	-	8.7	-	10.7
Φ_Δ	-	-	-	0.54

Table 1 A summary of the photophysical properties of the Tat-TPP conjugate. $\lambda_{abs\ Soret}$: the peak Soret band absorption; $\lambda_{abs\ Q}$: the peak Q band absorption in the red spectral region; λ_{ex}: the fluorescence excitation wavelength maxima ($\lambda_{emission}$ 651 nm); λ_{em}: the fluorescence emission wavelength maxima ($\lambda_{excitaion}$ 420 nm); τ_F: fluorescence lifetime; Φ_Δ: singlet oxygen quantum yield. ([a]: distilled water; [b]: methanol; [c]: DMPC liposomal solution; [d]: deuterated methanol).

3.4. Cellular uptake of Tat-TPP in comparison with $TPPS_{2a}$

Human squamous cell carcinoma HN5 cells were incubated with the Tat-TPP conjugate or the amphiphilic sulfonated derivative, $TPPS_{2a}$ and cellular fluorescence levels were compared as a function of time or concentration. Control cells without applied drug exhibited negligible fluorescence levels. As shown in Fig. 4A, time-dependent cell uptake was found for both photosensitisers. Higher fluorescence levels were measured in cells treated with Tat-TPP (1 μM) compared to $TPPS_{2a}$ (1.3 μM) at longer incubation times even though the concentration of Tat-TPP was slightly lower. The variation in cellular fluorescence versus concentration up to 5 μM recorded at 18 hr, the time-point used in subsequent PCI studies, shown in Fig. 4B. Above 1 μM, relatively little increase in fluorescence levels was observed. In addition, after 18hr incubation, the fluorescence intensity was measured to be three times higher in cells treated with 0.1 μM Tat-TPP, the concentration used in subsequent PCI studies, compared with $TPPS_{2a}$ using the same concentration.

To study the uptake mechanism of Tat-TPP and the possible involvement of endocytosis, which is temperature-dependent unlike passive transport, experiments using low temperature incubation were performed. The cellular uptake of Tat-TPP exhibits a temperature dependence, as shown in Fig. 4C. Incubation at 4 ºC resulted in a significant reduction of cellular uptake compared to incubation at 37 ºC ($p < 0.01$). The same behaviour was also observed in the cells incubated with $TPPS_{2a}$, which is known to be taken up via endocytosis [37].

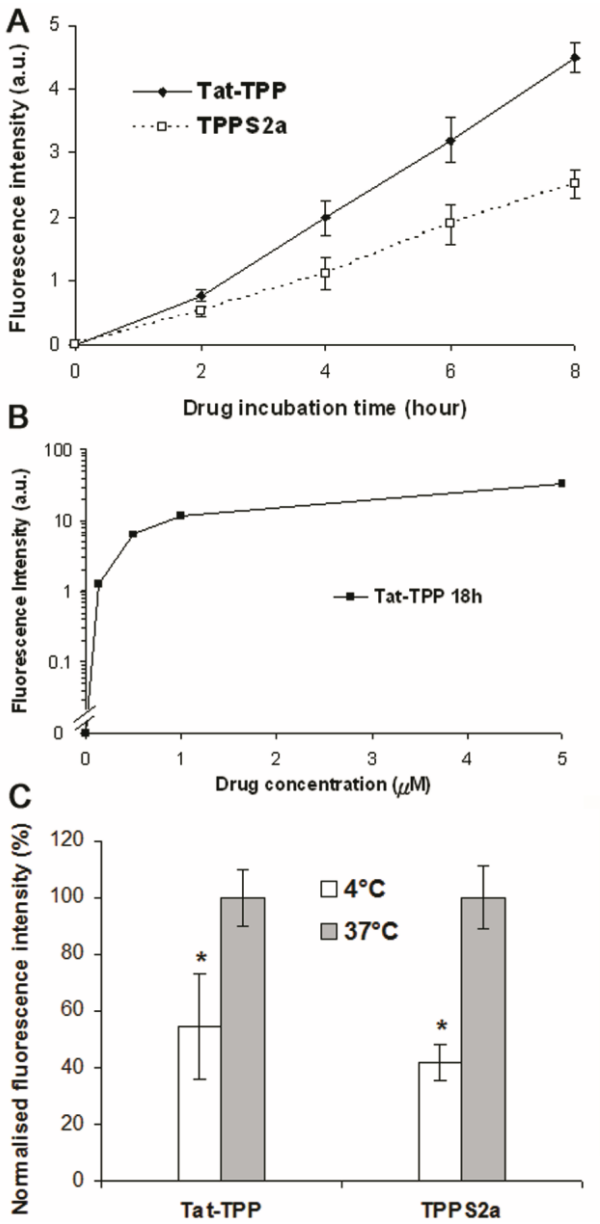

Fig. 4. Cellular fluorescence levels of Tat-TPP in comparison with $TPPS_{2a}$ in HN5 cells. A: Cells were incubated with Tat-TPP (1 μM) and $TPPS_{2a}$ (1.3 μM) for 8 hr. B: Cells were incubated with Tat-TPP (up to 5 μM) for 18hr. C: Normalised cellular fluorescence levels of Tat-TPP (1 μM) and $TPPS_{2a}$ (1.3 μM) at 4 ºC or 37 ºC after 1 hr incubation.

3.5. Subcellular localisation and light-induced redistribution of Tat-TPP using confocal microscopy

After 18hr incubation, a granular intracellular distribution of the Tat-TPP conjugate was observed by confocal microscopy (Fig. 5A), which became diffuse following prolonged light exposure (Fig. 5B). The exposure time needed to acquire the images was small (< 10 s) compared with the duration of the light exposure required to induce the redistribution (10 min). A slight increase of about 20 % in integrated cellular fluorescence intensity accompanied the redistribution which we have also observed in similar experiments using aluminium disulfonated phthalocyanine and is believed to result from the reduction in concentration self-quenching of fluorescence [43].

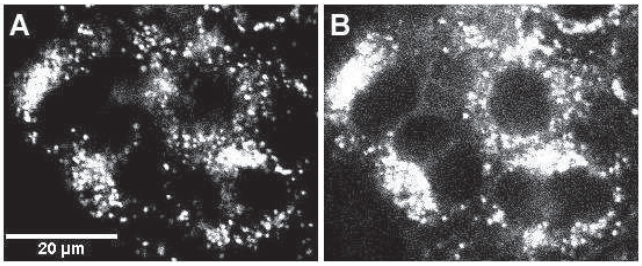

Fig. 5. Cellular distribution of Tat-TPP and the redistribution after irradiation on stage in HN5 cells by confocal microscopy. A: before light; B: 10 min light exposure. Light source: 543 nm confocal microscope laser. Cells were incubated with 2.5 µM Tat-TPP for 18 hr. Scale bar: 20 µm.

The subcelllular localisation of Tat-TPP (Fig. A and D) was investigated by co-labelling cells with LysoTracker Green (Fig. 6B) or MitoTracker Green (Fig. 6E), since a granular or punctate subcellular distribution can be associated with either lysosomal or mitochondrial uptake. As shown in the merged images Fig. 6C and 6F, most Tat-TPP was found co-localised with lysosomes (yellow). Less overlap was apparent using the mitochondrial probe.

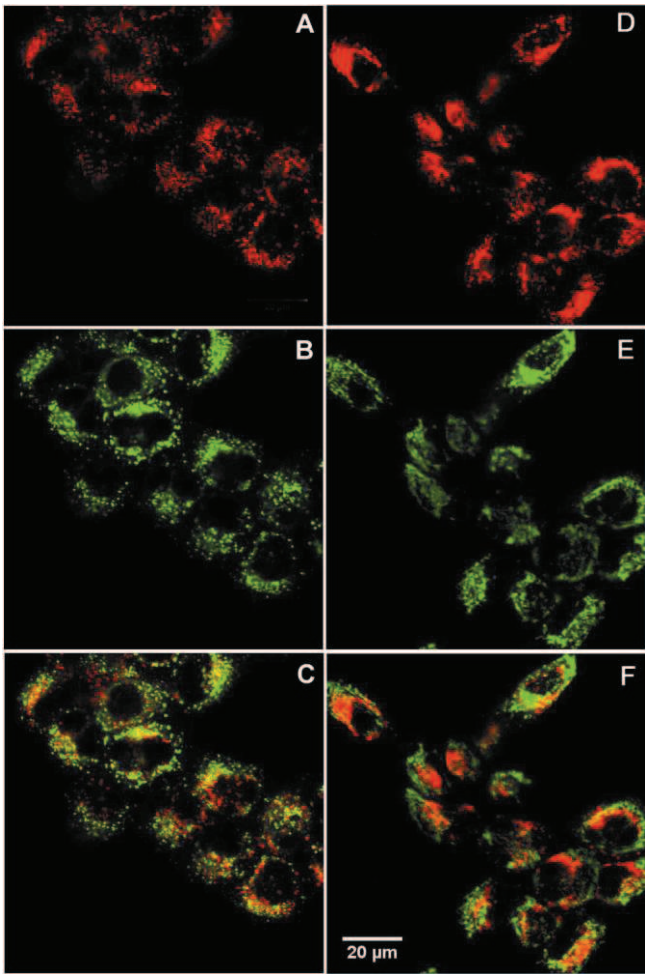

Fig. 6. Colocalisation studies of Tat-TPP versus LysoTracker Green or MitoTracker Green in HN5 cells by confocal microscopy. Cells were incubated 2.5 µM Tat-TPP for 18 hr. 50 nM of LysoTracker Green or MitoTracker Green was applied to cells 30 min before imaging. A and D: Tat-TPP; B: LysoTracker Green; C: merged A and B; E: MitoTracker Green; F: merged D and E. Scale bar: 20 µm.

3.6. Phototoxicity and the PCI effect of Tat-TPP combing saporin in HN5 cells

The phototoxicity of the Tat-TPP conjugate in HN5 cells was studied as a function of both incubation concentration (up to 0.2 μM) and different light exposures (Fig. 7, black, dark and light blue lines). The phototoxicity induced by Tat-TPP was found to increase with both the light and drug dose. Cell viability was reduced to 40 % and 25 % using the conjugate at concentration of 0.1 μM and 0.2 μM respectively after 3 min light exposure, which corresponds to a fluence of 1.3 J cm $^{-2}$ Control values without light exposure are given by the ordinate readings, which show that little dark toxicity was evident induced by the conjugate. Controls performed with light only showed no measureable reduction in viability.

Previous studies have shown that a sub-lethal combination of photosensitiser and light dose, corresponding to c. 50 % reduction in viability, is the optimal condition for PCI treatment [35,37]. The PCI effect in combination with saporin was therefore examined using a concentration of 0.1 μM and 3 minutes light exposure for the Tat-TPP conjugate. In Fig. 7, the solid purple and orange lines represent the cell viability after being treated with increasing doses of saporin alone (10 and 25 nM). Control values for saporin only without light exposure are given by the ordinate readings. After light exposure there was no significant enhancement in toxicity with saporin only, and the viability at the 3 min timepoint was measured as 56% for 10 nM saporin. However, significantly enhanced cell killing ($p < 0.001$) was demonstrated by PCI using Tat-TPP in combination with saporin at each dose (dotted lines), and for 10 nM the viability was reduced to 5%. In summary, using 10 nM saporin and 0.1 μM Tat-TPP, PCI treatment significantly reduced the cell viability by factors of 11.2 and 7.3 compared to saporin and Tat-TPP alone respectively after 3 min light exposure. PCI using the Tat-TPP conjugate therefore significantly enhanced the cytotoxicity induced by the type I RIP toxin, saporin.

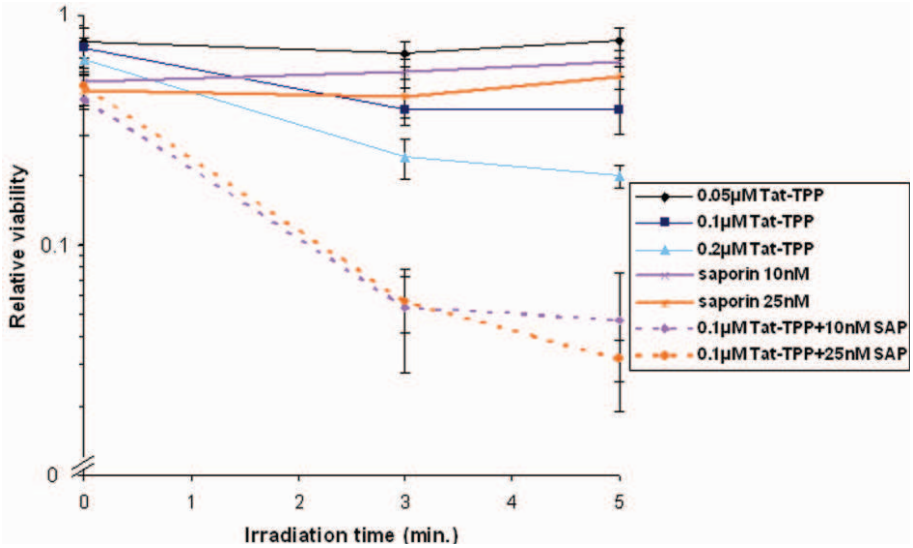

Fig. 7. Tat-TPP PDT (without saporin) and PCI effect (with saporin) in HN5 cells. Cells were incubated with 0.1 μM or 0.2 μM Tat-TPP, with or without saporin (10, 25 nM) for 18hr. Irradiation was carried out up to 5 min using a blue lamp. Cell viability was examined by the MTT assay 48 hr after exposure to light.

4. Discussion

In this study a cell penetrating peptide containing the core Tat sequence conjugated to a porphyrin (TPP) photosensitiser was investigated for photochemical internalisation (PCI), which is a site-specific technique for improving drug delivery. The key property required of a photosensitiser designed for PCI is the ability to localise specifically in endo/lysosomal membranes This is a key difference from photosensitisers designed for photodynamic therapy

where localisation in other subcellular compartments may confer an advantage (e.g. in mitochondria) rather than the specific endo/lysosomal localisation required for PCI. The efficacy of the water soluble peptide-porphyrin bioconjugate for PCI was investigated in a human head and neck squamous cell carcinoma cell line, which was selected on the basis that PCI may be suited to head and neck cancer therapy. Prior to the cellular studies, a series of spectroscopic and photophysical studies of the conjugate were carried out in different solvents, including a liposomal solution, to investigate its physicochemical properties. The Tat-TPP conjugate displayed typical fluorescence spectra in aqueous solution for a tetraphenyl porphyrin with two emission bands, but a red shift was observed in aqueous solution containing DMPC liposomes in both excitation and emission spectra (Fig. 3), which would be consistent with binding of the conjugate to the liposomal membrane. Such spectral shifts upon membrane binding of porphyrins have been reported in numerous studies [44,45]. This result would imply that the bioconjugate should also bind to cellular/organelle membranes, which is a key property required of photosensitisers used for PCI [46]. The fluorescence lifetime of Tat-TPP in methanol was measured as 8.7 ns compared to a value of 9.7 ns for $TPPS_4$ which is in good agreement with the result from another study [47]. The singlet oxygen yield of the Tat-TPP conjugate was determined in methanol, giving $\Phi_\Delta = 0.54$, which is close to a reported value of 0.56 for TPP [46], .

The cellular uptake of the Tat-TPP conjugate was investigated in the HN5 human squamous cell carcinoma line in comparison to $TPPS_{2a}$ which is an amphiphilic tetraphenyl porphyrin used for both PCI and PDT. The results in Fig. 4A show that the conjugate was taken up by cells efficiently with fluorescence levels comparable to those using a similar concentration of $TPPS_{2a}$. Incubation at 4ºC reduced the uptake of both photosensitisers, although to a lesser extent with the conjugate, which is consistent with the involvement of an energy-dependent endocytic mechanism of cellular uptake (Fig. 4C). The residual uptake of the conjugate at conjugate may be due to binding of the cationic Tat peptide to the cell membrane as previously proposed [46]. The subcellular distribution of the Tat-TPP conjugate was observed to be similar to $TPPS_{2a}$ (data not shown) exhibiting a granular pattern which became diffuse after light exposure (Fig. 5), which is consistent with the endo/lysosomal rupture mechanism required for PCI. Co-localisation studies with lysosomal and mitochondria probes showed that the conjugate appears to accumulate mainly in lysosomes as a consequence of endocytic cellular uptake. Since the molecular weight of the Tat conjugate is approx. 4000 Da, endocytic uptake would be expected for a molecule of this size. Overall, the results indicate that endocytosis is the main uptake mechanism of Tat-porphyrin conjugates, and that the conjugate is likely to be bound to the endo/lysosomal membrane instead of the aqueous lysosomal compartment based on the observation of membrane binding in the liposome studies. In a previous study, we investigated the photoinduced membrane permeation by the same Tat-porphyrin conjugate in relation to their antibacterial PDT effects [30]. Photo-induced release of carboxyfluorescein entrapped within unilamellar vesicles prepared from negatively charged lipids was observed, which mirrors the light-induced intracellular redistribution observed in the present study. Collectively, the experimental results presented here are in agreement with results of Vicente and co-workers that Tat-porphyrin conjugates are taken up efficiently by cells and can display an endo/lysosomal intracellular localisation [29,48,49]. Moreover, in another study it was found cationic porphyrins without the peptide component exhibited preferential mitochondrial uptake, which renders them unsuitable for PCI [49]. The serum stability of peptide-porphyrin conjugates [48] has also been investigated and it was found that these conjugates can undergo partially hydrolysis by proteolytic enzymes after 24 hr incubation. It is possible that the conjugate used here may undergo similar processes, although this should have no effect upon the efficiency of subsequent photoinduced membrane damage, and further studies need to be carried out on the optimum incubation time. The choice of the 18 hr incubation time used here was based on previous PCI studies with other porphyrin photosensitisers.

To test whether the Tat-TPP conjugate has the potential for PCI, its phototoxicity was examined in the HN5 line in combination with the macromolecular toxin, saporin, As shown in

Fig. 7, Tat-TPP induced phototoxicity using low concentrations, and a sub-lethal combination of photosensitiser and light dose suitable for PCI was identified. The significantly enhanced cell killing achieved by combing low concentrations of saporin with a sub-lethal light dose demonstrated that the Tat-TPP conjugate is capable of acting as a PCI photosensitiser, since the same concentrations of saporin used without illumination are non-toxic. The PCI effect using Tat-TPP was found to be comparable to another PCI photosensitiser $TPPS_{2a}$ in which the combination of sub-lethal PDT and saporin treatment induced 95 % reduction of cell viability [35,36]. The concentration employed here for the Tat-TPP conjugate of 0.1 μM is comparable to concentrations employed for PCI with $TPPS_{2a}$. However since we observed higher cellular fluorescence levels using the conjugate than $TPPS_{2a}$ (section 3.4), future studies may therefore be able to employ even lower concentrations of the conjugate.

The present study is the first attempt to incorporate the cell penetrating peptide-photosensitiser conjugation strategy for PCI-enhanced delivery of a macromolecular toxin. The growing number of cell penetrating peptides that are becoming available [4,50] together with efforts to incorporate tumour targeting, add to the versatility of this approach. In summary, it has been demonstrated that a CPP-photosensitiser conjugate exhibits favourable properties for PCI. Firstly, the combination of good photophysical properties, water solubility yet sufficient amphiphilicity to localise in membranes. Secondly, efficient cellular uptake and low dark toxicity, and finally the synergistic PCI cytotoxicity in combination with saporin. A further advantage is that conjugation to a CPP allows photosensitisers like TPPs, with good photophysical properties to be used, whereas on their own they are not suitable for PCI applications since they are water-insoluble, and not amphiphilic. Not surprisingly, some studies have pointed out that Tat peptide bioconjugates might result differently *in vitro* and *in vivo* [51,52], therefore future in vivo studies need to carefully consider the differences in experimental settings. Although limited cell specificity has been a drawback in the use of CPPs such as the Tat sequence [53], although this may improve in future, PCI selectivity can also be achieved through its light-activated site specificity so that the therapeutic effects are confined to the area exposed to light.

Acknowledgements
This study was supported in part by grants from Biotechnology and Biological Sciences Research Council grants BBD0127831 (IM Eggleston), and BBD0113291 (M Wilson, AJ MacRobert). We are grateful for assistance from Dr Ludovic Bourré in the preparation of the liposomes.

Figure captions:

Fig. 1. Structures of modified tetraphenylporphyrin **1** and Tat-tetraphenylporphyrin (Tat-TPP) bioconjugate **2**.

Fig. 2. Absorption spectrum of 5 μM Tat-TPP conjugate in aqueous solution. Inset: the Q band region from 450 nm to 700 nm.

Fig. 3. Fluorescence spectrum of 2.5 μM Tat-TPP in aqueous and DMPC liposomal solutions. A: Emission spectra ($\lambda_{excitation}$ 420 nm); B: Excitation spectra ($\lambda_{emission}$ 651 nm). The emission spectra were corrected for the variation of detector sensitivity with wavelength. Front surface excitation/detection geometry was employed to minimise self-absorption.

Fig. 4. Cellular fluorescence levels of Tat-TPP in comparison with $TPPS_{2a}$ in HN5 cells. A: Cells were incubated with Tat-TPP (1 μM) and $TPPS_{2a}$ (1.3 μM) for 8 hr. B: Cells were incubated with Tat-TPP (up to 5 μM) for 18hr. C: Normalised cellular fluorescence levels of Tat-TPP (1 μM) and $TPPS_{2a}$ (1.3 μM) at 4 ºC or 37 ºC after 1 hr incubation.

Fig. 5. Cellular distribution of Tat-TPP and the redistribution after irradiation on stage in HN5 cells by confocal microscopy. A: before light; B: 10 min light exposure. Light source: 543nm confocal microscope laser. Cells were incubated with 2.5μM Tat-TPP for 18 hr. Scale bar: 20 μm.

Fig. 6. Colocalisation studies of Tat-TPP versus LysoTracker Green or MitoTracker Green in HN5 cells by confocal microscopy. Cells were incubated 2.5μM Tat-TPP for 18hr. 50 nM of LysoTracker Green or MitoTracker Green was applied to cells 30 min before imaging. A and D: Tat-TPP; B: LysoTracker Green; C: merged A and B; E: MitoTracker Green; F: merged D and E. Scale bar: 20 μm.

Fig. 7. Tat-TPP PDT (without saporin) and PCI effect (with saporin) in HN5 cells. Cells were incubated with 0.1 μM or 0.2 μM Tat-TPP, with or without saporin (10, 25 nM) for 18hr. Irradiation was carried out up to 5 min using a blue lamp. Cell viability was examined by the MTT assay 48 hr after exposure to light.

Table captions:

Table 1 A summary of the photophysical properties of the Tat-TPP conjugate. $\boldsymbol{\lambda_{abs\ Soret}}$: the peak Soret band absorption; $\boldsymbol{\lambda_{abs\ Q}}$: the peak Q band absorption in the red spectral region; $\boldsymbol{\lambda_{ex}}$: the fluorescence excitation wavelength maxima ($\lambda_{emission}$ 651 nm); $\boldsymbol{\lambda_{em}}$: the fluorescence emission wavelength maxima ($\lambda_{excitaion}$ 420 nm); $\boldsymbol{\tau_F}$: fluorescence lifetime; $\boldsymbol{\Phi_\Delta}$: singlet oxygen quantum yield. ([a]: distilled water; [b]: methanol; [c]: DMPC liposomal solution; [d]: deuterated methanol).

Reference List

[1] J. Woodhams, P.J. Lou, P.K. Selbo, A. Mosse, D. Oukrif, A. MacRobert, M. Novelli, Q. Peng, K. Berg, and S.G. Bown, Intracellular re-localisation by photochemical internalisation enhances the cytotoxic effect of gelonin - Quantitative studies in normal rat liver, Journal of Controlled Release, 142 (2010) 347-353.

[2] P.K. Selbo, A. Weyergang, A. Hogset, O.J. Norum, M.B. Berstad, M. Vikdal, and K. Berg, Photochemical internalization provides time- and space-controlled endolysosomal escape of therapeutic molecules, J. Control Release, (2010).

[3] J.T.-W. Wang, J.H. Woodhams, A.J. MacRobert, S.G. Bown, and K. Berg, Photodynamic Drug Delivery, CRC Handbook of Organic Photochemistry and Photobiology, Third Edition, CRC Press, 2011.

[4] K.M. Stewart, K.L. Horton, and S.O. Kelley, Cell-penetrating peptides as delivery vehicles for biology and medicine, Organic & Biomolecular Chemistry, 6 (2008) 2242-2255.

[5] M. Green and P.M. Loewenstein, Autonomous functional domains of chemically synthesized human immunodeficiency virus tat trans-activator protein, Cell, 55 (1988) 1179-1188.

[6] A.D. Frankel and C.O. Pabo, Cellular uptake of the tat protein from human immunodeficiency virus, Cell, 55 (1988) 1189-1193.

[7] S. Ruben, A. Perkins, R. Purcell, K. Joung, R. Sia, R. Burghoff, W.A. Haseltine, and C.A. Rosen, Structural and functional characterization of human immunodeficiency virus tat protein, J. Virol., 63 (1989) 1-8.

[8] M. Kuppuswamy, T. Subramanian, A. Srinivasan, and G. Chinnadurai, Multiple functional domains of Tat, the trans-activator of HIV-1, defined by mutational analysis, Nucleic Acids Res., 17 (1989) 3551-3561.

[9] E. Vives, P. Brodin, and B. Lebleu, A truncated HIV-1 Tat protein basic domain rapidly translocates through the plasma membrane and accumulates in the cell nucleus, J. Biol. Chem., 272 (1997) 16010-16017.

[10] P. Lundberg and U. Langel, A brief introduction to cell-penetrating peptides, Journal of Molecular Recognition, 16 (2003) 227-233.

[11] D.R. Gius, S.A. Ezhevsky, M. Becker-Hapak, H. Nagahara, M.C. Wei, and S.F. Dowdy, Transduced p16INK4a Peptides Inhibit Hypophosphorylation of the Retinoblastoma Protein and Cell Cycle Progression Prior to Activation of Cdk2 Complexes in Late G1, Cancer Res, 59 (1999) 2577-2580.

[12] V.P. Torchilin, R. Rammohan, V. Weissig, and T.S. Levchenko, TAT peptide on the surface of liposomes affords their efficient intracellular delivery even at low temperature and in the presence of metabolic inhibitors, Proc. Natl. Acad. Sci. U. S. A, 98 (2001) 8786-8791.

[13] E. Vives, C. Granier, P. Prevot, and B. Lebleu, Structure-activity relationship study of the plasma membrane translocating potential of a short peptide from HIV-1 Tat protein, Letters in Peptide Science, 4 (1997) 429-436.

[14] P.A. Wender, D.J. Mitchell, K. Pattabiraman, E.T. Pelkey, L. Steinman, and J.B. Rothbard, The design, synthesis, and evaluation of molecules that enable or enhance cellular uptake: peptoid molecular transporters, Proc. Natl. Acad. Sci. U. S. A, 97 (2000) 13003-13008.

[15] S. Sandgren, F. Cheng, and M. Belting, Nuclear Targeting of Macromolecular Polyanions by an HIV-Tat Derived Peptide. Role for cell-surface proteoglycans., J. Biol. Chem., 277 (2002) 38877-38883.

[16] S. Console, C. Marty, C. Garcia-Echeverria, R. Schwendener, and K. Ballmer-Hofer, Antennapedia and HIV Transactivator of Transcription (TAT) "Protein Transduction Domains" Promote Endocytosis of High Molecular Weight Cargo upon Binding to Cell Surface Glycosaminoglycans, J. Biol. Chem., 278 (2003) 35109-35114.

[17] J.P. Richard, K. Melikov, E. Vives, C. Ramos, B. Verbeure, M.J. Gait, L.V. Chernomordik, and B. Lebleu, Cell-penetrating Peptides. A reevaluation of the mechanism of cellular uptake, J. Biol. Chem., 278 (2003) 585-590.

[18] V.P. Torchilin, Tat peptide-mediated intracellular delivery of pharmaceutical nanocarriers, Advanced Drug Delivery Reviews, 60 (2008) 548-558.

[19] A. Vendeville, F. Rayne, A. Bonhoure, N. Bettache, P. Montcourrier, and B. Beaumelle, HIV-1 Tat Enters T Cells Using Coated Pits before Translocating from Acidified Endosomes and Eliciting Biological Responses, Mol. Biol. Cell, 15 (2004) 2347-2360.

[20] A. Fittipaldi, A. Ferrari, M. Zoppe, C. Arcangeli, V. Pellegrini, F. Beltram, and M. Giacca, Cell membrane lipid rafts mediate caveolar endocytosis of HIV-1 Tat fusion proteins, J. Biol. Chem., 278 (2003) 34141-34149.

[21] J.S. Wadia, R.V. Stan, and S.F. Dowdy, Transducible TAT-HA fusogenic peptide enhances escape of TAT-fusion proteins after lipid raft macropinocytosis, Nat Med, 10 (2004) 310-315.

[22] H. Brooks, B. Lebleu, and E. Vives, Tat peptide-mediated cellular delivery: back to basics, Adv. Drug Deliv. Rev., 57 (2005) 559-577.

[23] S.R. Schwarze, A. Ho, A. Vocero-Akbani, and S.F. Dowdy, In Vivo Protein Transduction: Delivery of a Biologically Active Protein into the Mouse, Science, 285 (1999) 1569-1572.

[24] S.B. Brown, E.A. Brown, and I. Walker, The present and future role of photodynamic therapy in cancer treatment, Lancet Oncol., 5 (2004) 497-508.

[25] L. Chaloin, P. Bigey, C. Loup, M. Marin, N. Galeotti, M. Piechaczyk, F. Heitz, and B. Meunier, Improvement of porphyrin cellular delivery and activity by conjugation to a carrier peptide, Bioconjug. Chem., 12 (2001) 691-700.

[26] N. Thomas, M. Pernot, R. Vanderesse, P. Becuwe, E. Kamarulzaman, D. Da Silva, A. François, C. Frochot, F. Guillemin, and M. Barberi-Heyob, Photodynamic therapy targeting neuropilin-1: Interest of pseudopeptides with improved stability properties, Biochemical Pharmacology, 80 (2010) 226-235.

[27] M.J. Dixon, L. Bourré, A.J. MacRobert, and I.M. Eggleston, Novel prodrug approach to photodynamic therapy: Fmoc solid-phase synthesis of a cell permeable peptide incorporating 5-aminolaevulinic acid, Bioorganic & Medicinal Chemistry Letters, 17 (2007) 4518-4522.

[28] M. Sibrian-Vazquez, T.J. Jensen, R.P. Hammer, and M.G. Vicente, Peptide-mediated cell transport of water soluble porphyrin conjugates, J. Med Chem., 49 (2006) 1364-1372.

[29] I. Sehgal, M. Sibrian-Vazquez, and M.G. Vicente, Photoinduced cytotoxicity and biodistribution of prostate cancer cell-targeted porphyrins, J. Med Chem., 51 (2008) 6014-6020.

[30] L. Bourré, F. Giuntini, I.M. Eggleston, C.A. Mosse, A.J. MacRobert, and M. Wilson, Effective photoinactivation of Gram-positive and Gram-negative bacterial strains using an HIV-1 Tat peptide-porphyrin conjugate, Photochem. Photobiol. Sci., 9 (2010) 1613-1620.

[31] P.J. Lou, P.S. Lai, M.J. Shieh, A.J. MacRobert, K. Berg, and S.G. Bown, Reversal of doxorubicin resistance in breast cancer cells by photochemical internalization, Int. J. Cancer, 119 (2006) 2692-2698.

[32] D.K. Adigbli, D.G. Wilson, N. Farooqui, E. Sousi, P. Risley, I. Taylor, A.J. MacRobert, and M. Loizidou, Photochemical internalisation of chemotherapy potentiates killing of multidrug-resistant breast and bladder cancer cells, Br. J. Cancer, 97 (2007) 502-512.

[33] T. Shiraishi and P.E. Nielsen, Photochemically enhanced cellular delivery of cell penetrating peptide-PNA conjugates, FEBS Lett., 580 (2006) 1451-1456.

[34] M.G. Battelli, Cytotoxicity and toxicity to animals and humans of ribosome-inactivating proteins, Mini. Rev. Med Chem., 4 (2004) 513-521.

[35] A. Weyergang, P.K. Selbo, and K. Berg, Photochemically stimulated drug delivery increases the cytotoxicity and specificity of EGF-saporin, J. Control Release, 111 (2006) 165-173.

[36] W.L. Yip, A. Weyergang, K. Berg, H.H. Tonnesen, and P.K. Selbo, Targeted delivery and enhanced cytotoxicity of cetuximab-saporin by photochemical internalization in EGFR-positive cancer cells, Mol. Pharm., 4 (2007) 241-251.

[37] P.K. Selbo, K. Sandvig, V. Kirveliene, and K. Berg, Release of gelonin from endosomes and lysosomes to cytosol by photochemical internalization, Biochim. Biophys. Acta, 1475 (2000) 307-313.

[38] S. Santra, H. Yang, J.T. Stanley, P.H. Holloway, B.M. Moudgil, G. Walter, and R.A. Mericle, Rapid and effective labeling of brain tissue using TAT-conjugated CdS[ratio]Mn/ZnS quantum dots, Chem. Commun., (2005) 3144-3146.

[39] M.J. Hope, R. Nayar, L.D. Mayer, and P.R. Cullis, Reduction of liposome size and preparation of unilamellar vesicles by extrusion techniques., in: G. Gregoriadis (Ed.), Liposome Technology, Vol. 1. CRC Press, Boca Raton, FL, 1992, pp. 123-139.

[40] C. Tanielian, C. Wolff, and M. Esch, Singlet oxygen production in water: Aggregation and charge-transfer effects, Journal of Physical Chemistry, 100 (1996) 6555-6560.

[41] R.W. Redmond and J.N. Gamlin, A compilation of singlet oxygen yields from biologically relevant molecules, Photochem. Photobiol., 70 (1999) 391-475.

[42] C. Cantau, T. Pigot, N. Manoi, E. Oliveros, and S. Lacombe, Singlet oxygen in microporous silica xerogel: Quantum yield and oxidation at the gas-solid interface, Chemphyschem, 8 (2007) 2344-2353.

[43] L. Kunz, J.P. Connelly, J.H. Woodhams, and A.J. MacRobert, Photodynamic modification of disulfonated aluminium phthalocyanine fluorescence in a macrophage cell line, Photochem. Photobiol. Sci., 6 (2007) 940-948.

[44] D. Kessel and E. Rossi, Determinants of Porphyrin-Sensitized Photo-Oxidation Characterized by Fluorescence and Absorption-Spectra, Photochemistry and Photobiology, 35 (1982) 37-41.

[45] F. Ricchelli, Photophysical properties of porphyrins in biological membranes, Journal of Photochemistry and Photobiology B: Biology, 29 (1995) 109-118.

[46] C. Tanielian and C. Wolff, Porphyrin-Sensitized Generation of Singlet Molecular-Oxygen - Comparison of Steady-State and Time-Resolved Methods, Journal of Physical Chemistry, 99 (1995) 9825-9830.

[47] M.A. Castriciano, M.G. Donato, V. Villari, N. Micali, A. Romeo, and L.M. Scolaro, Surfactant-like behavior of short-chain alcohols in porphyrin aggregation, J. Phys. Chem. B, 113 (2009) 11173-11178.

[48] M. Sibrian-Vazquez, T.J. Jensen, and M.G. Vicente, Synthesis, characterization, and metabolic stability of porphyrin-peptide conjugates bearing bifunctional signaling sequences, J. Med Chem., 51 (2008) 2915-2923.

[49] M. Sibrian-Vazquez, E. Hao, T.J. Jensen, and M.G. Vicente, Enhanced cellular uptake with a cobaltacarborane-porphyrin-HIV-1 Tat 48-60 conjugate, Bioconjug. Chem., 17 (2006) 928-934.

[50] T.J. Jensen, M.G.H. Vicente, R. Luguya, J. Norton, F.R. Fronczek, and K.M. Smith, Effect of overall charge and charge distribution on cellular uptake, distribution and phototoxicity of cationic porphyrins in HEp2 cells, Journal of Photochemistry and Photobiology B-Biology, 100 (2010) 100-111.

[51] N.J. Caron, Y. Torrente, G. Camirand, M. Bujold, P. Chapdelaine, K. Leriche, N. Bresolin, and J.P. Tremblay, Intracellular Delivery of a Tat-eGFP Fusion Protein into Muscle Cells, Mol Ther, 3 (2001) 310-318.

[52] U. Niesner, C. Halin, L. Lozzi, M. Gunthert, P. Neri, H. Wunderli-Allenspach, L. Zardi, and D. Neri, Quantitation of the tumor-targeting properties of antibody fragments conjugated to cell-permeating HIV-1 TAT peptides, Bioconjugate Chemistry, 13 (2002) 729-736.

[53] E. Vives, Present and future of cell-penetrating peptide mediated delivery systems: "is the Trojan horse too wild to go only to Troy?", J. Control Release, 109 (2005) 77-85.

Table 1

	dH_2O[a]	MeOH[b]	DMPC[c]	MeOD[d]
$\lambda_{abs\ Soret}$ (nm)	418	414	-	-
$\lambda_{abs\ Q}$ (nm)	642	645	-	-
λ_{ex} (nm)	417	-	420	-
λ_{em} (nm)	652, 714	-	655, 721	-
τ_F (ns)	-	8.7	-	10.7
Φ_Δ	-	-	-	0.54

Table 1 A summary of the photophysical properties of the Tat-TPP conjugate. $\lambda_{abs\ Soret}$: the peak Soret band absorption; $\lambda_{abs\ Q}$: the peak Q band absorption in the red spectral region; λ_{ex}: the fluorescence excitation wavelength maxima ($\lambda_{emission}$ 651nm); λ_{em}: the fluorescence emission wavelength maxima ($\lambda_{excitaion}$ 420nm); τ_F: fluorescence lifetime; Φ_Δ: singlet oxygen quantum yield. ([a]: distilled water; [b]: methanol; [c]: DMPC liposomal solution; [d]: deuterated methanol).

Figure 1

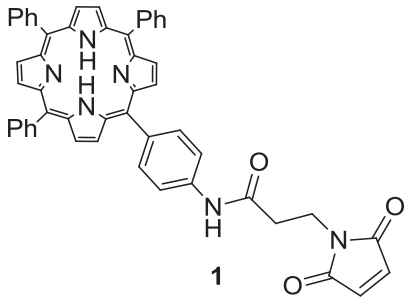

1

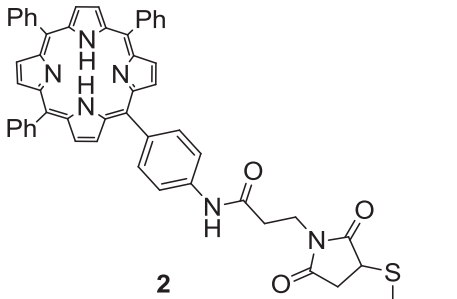

2

GRKKRRQRRRGYKC-NH_2

Figure 2 and 3

Fig. 2

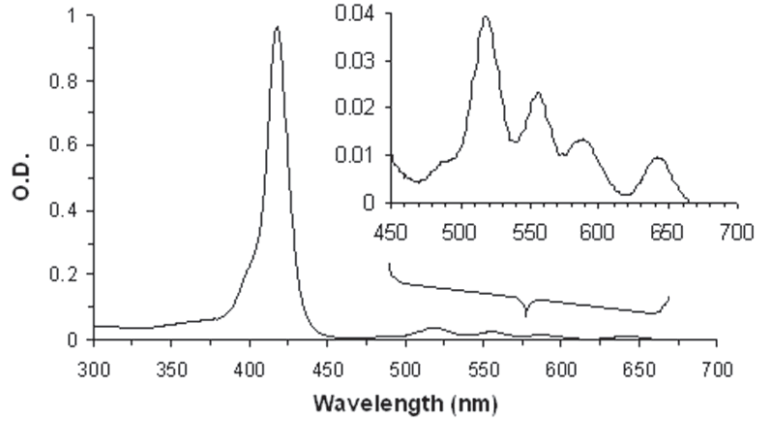

Fig. 3

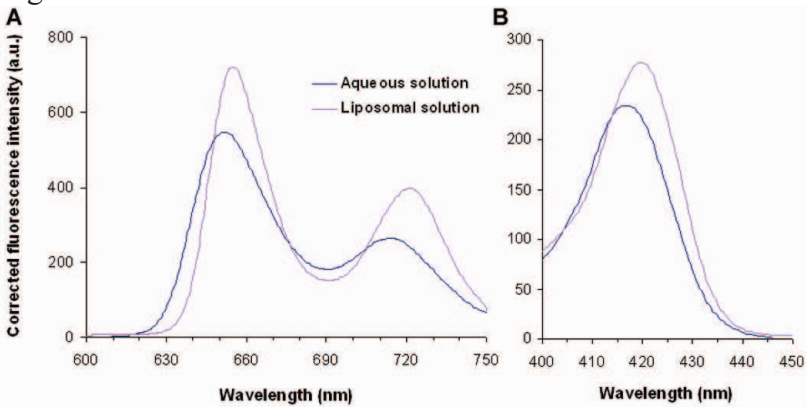

Figure 4

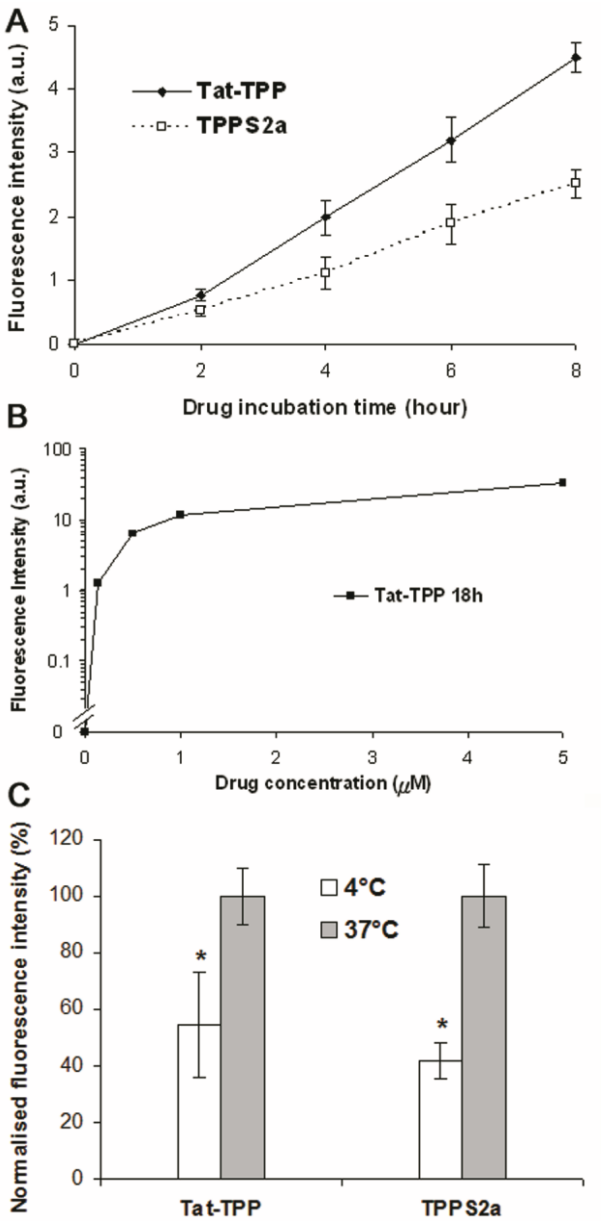
A
Fluorescence intensity (a.u.)
Tat-TPP
TPPS2a
Drug incubation time (hour)
B
Fluorescence Intensity (a.u.)
Tat-TPP 18h
Drug concentration (μM)
C
Normalised fluorescence intensity (%)
4°C
37°C
Tat-TPP
TPPS2a

Figure 5 and 6

Fig. 5

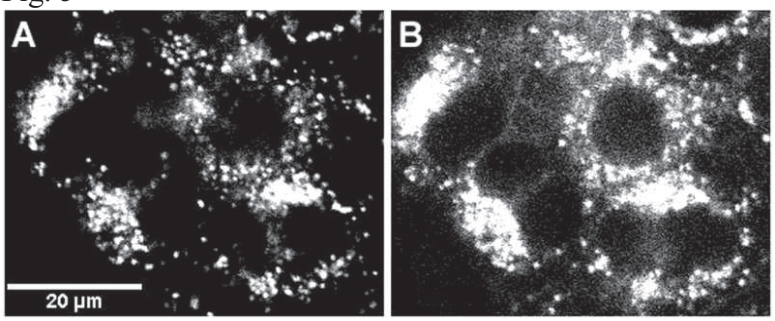

Fig. 6

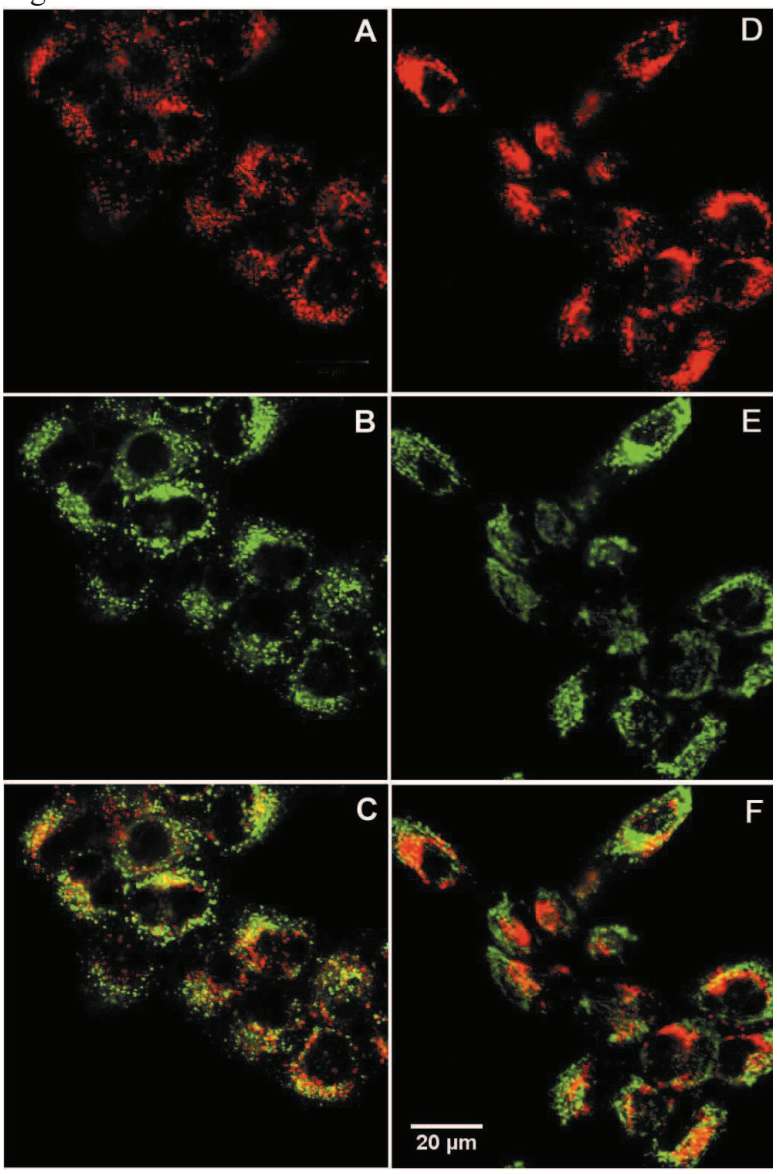

Figure 7

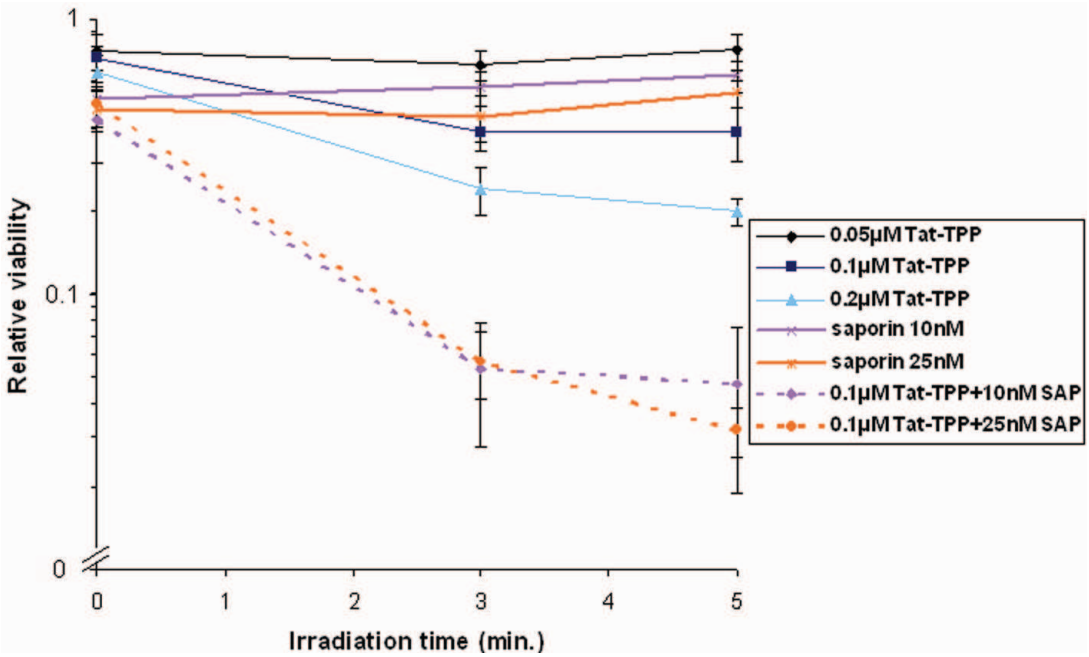
Relative viability
1
0.1
0
0
1
2
3
4
5
Irradiation time (min.)
0.05μM Tat-TPP
0.1μM Tat-TPP
0.2μM Tat-TPP
saporin 10nM
saporin 25nM
0.1μM Tat-TPP+10nM SAP
0.1μM Tat-TPP+25nM SAP